

Application of empirical interatomic potentials to liquid Si

Manabu Ishimaru, Kou Yoshida, and Teruaki Motooka

Department of Materials Science and Engineering, Kyushu University, Hakozaki, Fukuoka 812-81, Japan

(Received 15 August 1995)

Structural and dynamical properties of liquid Si (*l*-Si) have been investigated by molecular-dynamics calculations using the Tersoff potential. The pair-correlation function $g(r)$, bond-angle distribution function $g(\theta)$, and velocity autocorrelation function $Z(t)$ were calculated and compared with those of *l*-Si generated by the Stillinger-Weber (SW) potential and *ab initio* calculations reported previously. The Tersoff liquid reproduces $g(r)$ obtained by the SW potential and *ab initio* calculations except for a slight quantitative difference. On the other hand, $g(\theta)$ of the Tersoff liquid is entirely different from that of the SW liquid, but it is similar to the result of the *ab initio* approach. These results suggest that the Tersoff potential describes the features of static structures of *l*-Si, though this potential overestimates greatly the melting point. The Tersoff potential yields a similar tendency to the dynamical properties obtained by *ab initio* simulation, but some discrepancies exist, e.g., the period of oscillation in $Z(t)$.

I. INTRODUCTION

The Czochralski growth of single-crystal Si (*c*-Si) from liquid Si (*l*-Si) is a key technology in semiconductor processing. It is well known that defect formation in the obtained crystals depends sensitively on the growth conditions such as crystal growth rates and temperature gradients at the *c*-Si and *l*-Si interface. Therefore, optimization of these processing parameters is required for the production of high-quality *c*-Si, and extensive experimental investigations are continued.^{1,2} However, the optimum conditions are generally determined empirically, since the high melting temperature makes it difficult to analyze the growth mechanism. In order to obtain information on the behavior of the liquid phase during the crystal growth, the application of computer simulations to this field is very useful. Although great progress has been achieved in *ab initio* simulation methods for atomic-scale studies,³ these methods are still difficult to apply for large-scale systems. Therefore, various empirical interatomic potentials for Si have been proposed for the last decade.⁴⁻⁸

An empirical potential constructed by Stillinger and Weber⁴ (SW) includes two- and three-body interaction terms and it was parametrized on the basis of crystalline and liquid-phase data for Si. The SW potential has been widely used in molecular-dynamics (MD) studies of the liquid phase.^{4,9-13} The calculated pair-correlation function and its Fourier transform are in good agreement with experiments.¹⁴ Therefore, this potential has been considered to well reproduce the structural features of *l*-Si. However, Stich, Car, and Parrinello¹⁵ recently carried out an *ab initio* MD simulation of *l*-Si and pointed out that a higher-order correlation function such as the bond-angle distribution function is different from that of the SW liquid. The result suggests that the SW potential is not enough for the structural analysis of *l*-Si.

Tersoff^{5,16} has developed a different type of empirical interatomic potential for covalent solids. This potential is written as a Morse pairwise potential, but its attractive term depends on the local environment of a specific atomic pair which effectively includes many-body interactions. The adjustable parameters were determined by fitting to a database

containing the cohesive energy, lattice constant, and bulk modulus of the diamond structure and the cohesive energy of Si₂ and bulk polytypes of Si. It should be noted that the Tersoff potential is not adjusted to fit to any liquid-phase data. The Tersoff liquid has not been fully explored, since the solid-liquid transition in this case occurs at about 3000 K, almost twice the experimental value. In addition, only the pair-correlation function of the atomic configuration is examined in *l*-Si with the Tersoff model,^{5,11} and no further investigations have been conducted for the analysis of the higher-order correlation and dynamical properties.

In the present study, we applied the Tersoff potential to *l*-Si in order to examine the features of the liquid, using MD simulations. The physical properties of generated *l*-Si were compared with *ab initio* MD results and the results using the SW potential, and the validity of both empirical potentials was discussed.

II. SIMULATION PROCEDURE

The MD calculations were performed under constant *volume* and *temperature* conditions. We considered $N=512$ atoms in a cubic cell with periodic boundary conditions. The volume of the cell was fixed at 9261 Å³ so that the density is 2.57 g/cm³, which agrees with the density of *l*-Si. The atoms were at first placed on the diamond lattice sites and then initial velocities were randomly given. Then the system was heated up by rescaling the velocities of the particles. In the present study, we used the SW and Tersoff potentials with the parameters described in Refs. 17 and 16, respectively. The equations of motion were integrated using a velocity-Verlet algorithm¹⁸ with a time step $\Delta t=2\times 10^{-3}$ ps. The MD simulations were carried out for 30 000 Δt (60 ps), and the system was found to reach equilibrium during this period as judged by the total energies. The static and dynamic properties obtained for *l*-Si were compared with the results of experiments and *ab initio* calculations previously reported.

III. RESULTS

A. Structural properties of liquid Si

In our MD simulations using the SW and Tersoff potentials, the solid-liquid phase transition occurred at about 1400

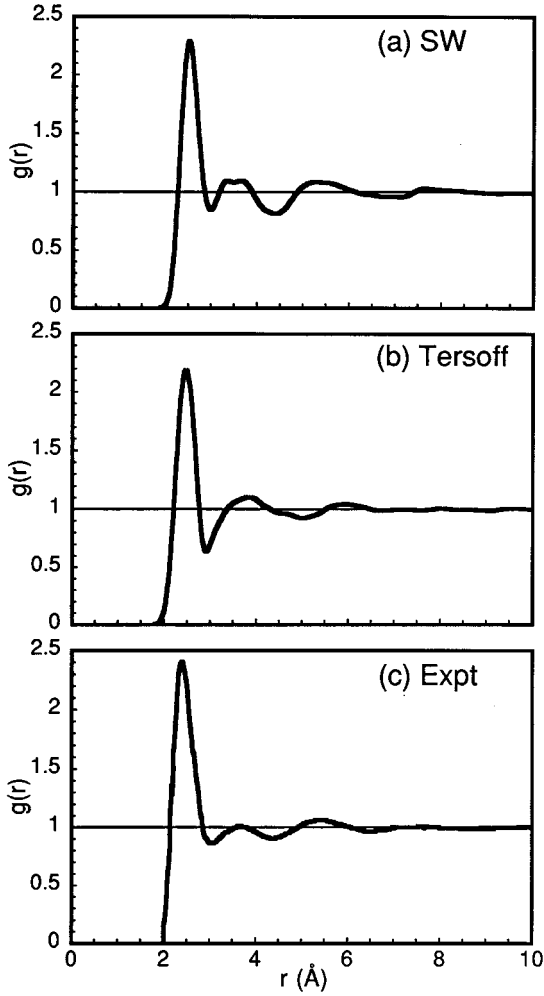


FIG. 1. Pair-correlation functions $g(r)$ for l -Si obtained from MD simulations using (a) SW and (b) Tersoff potentials. The experimental data from Ref. 11 are also indicated in (c). The simulated temperatures of (a) and (b) are 1700 and 3300 K, respectively. The $g(r)$ of SW liquid is in good agreement with the one obtained experimentally. Tersoff liquid, on the other hand, has a deep first minimum in (b).

and 2750 K, respectively. The melting temperature of the SW model in this work is lower than that originally reported by SW,⁴ since the density of the present system is larger than that used in the previous study. The calculated value of latent heat was 45.4 kJ/mol for the Tersoff potential. This value is close to the experimental value of 50.6 kJ/mol.¹⁹ We chose the simulated temperatures of 1700 and 3000 K in our MD calculations of the SW and Tersoff liquids, respectively, to ensure complete melting states. The discrepancy in the melting point between the simulations and experiments may not be important for our primary purpose to examine the liquid structures.

Figures 1(a) and 1(b) show the pair-correlation functions $g(r)$ of atomic configurations obtained at 1700 and 3000 K, respectively. These functions were obtained by averaging over 200 configurations during $200\Delta t$ (0.4 ps). This averaging time is considered long enough, because the correlation of atomic motion vanishes beyond 0.2 ps, as mentioned in Sec. III B. The positions of first and second peaks are almost

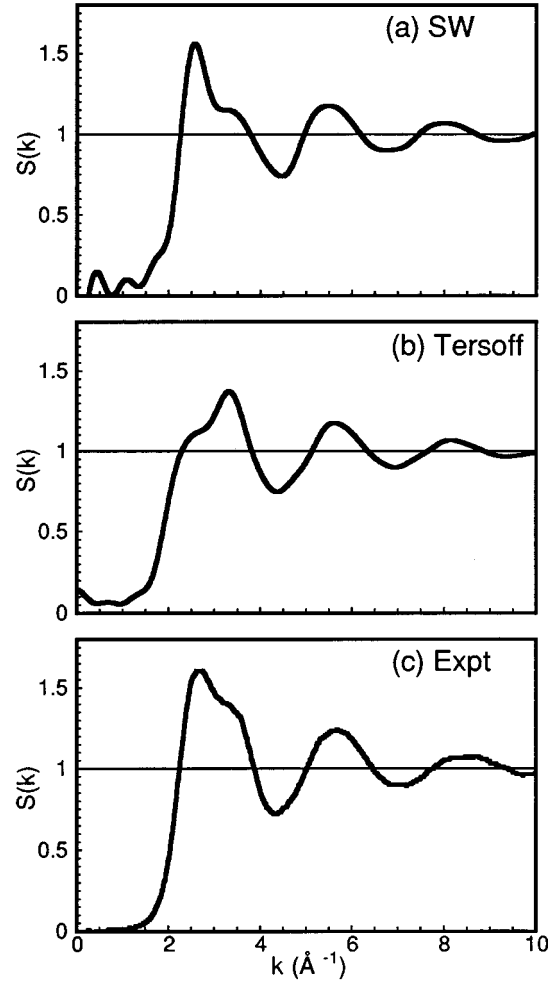


FIG. 2. Static structure factors $S(k)$ of l -Si resulting from (a) SW and (b) Tersoff potentials. Note the appearance of the asymmetric first peak. The shoulders are the high- and low-angle sides for (a) and (b), respectively. The former coincides with x-ray-diffraction experiments (c) of Ref. 11, but the latter is similar to the $S(k)$ obtained from a supercooled l -Si.

the same in both cases, but a quantitative difference exists. The depth of first minimum in Fig. 1(b) is appreciably deep, as compared with that of the experimentally obtained $g(r)$ shown in Fig. 1(c).¹⁴ The appearance of the deep first minimum can be attributed to the short cutoff distance of the potential, as Tersoff has previously reported.⁵

To compare with the available data of x-ray-diffraction experiments,¹⁴ the static structure factors $S(k)$ are calculated by Fourier transforming $g(r)$,

$$S(k) = 1 + 4\pi\rho_0 \int_0^\infty r^2 \{g(r) - 1\} \frac{\sin(kr)}{kr} dr. \quad (1)$$

Here, ρ_0 is the average number density of atoms and k is the wave number of the diffracted wave. Figures 2(a) and 2(b) demonstrate $S(k)$ corresponding to the $g(r)$ of Figs. 1(a) and 1(b), respectively. Again, the peak positions in Figs. 2(a) and 2(b) are in good agreement with the experimental data shown in Fig. 2(c).¹⁴ It is clearly seen that the first peak is asymmetric, and this has been known to be a characteristic

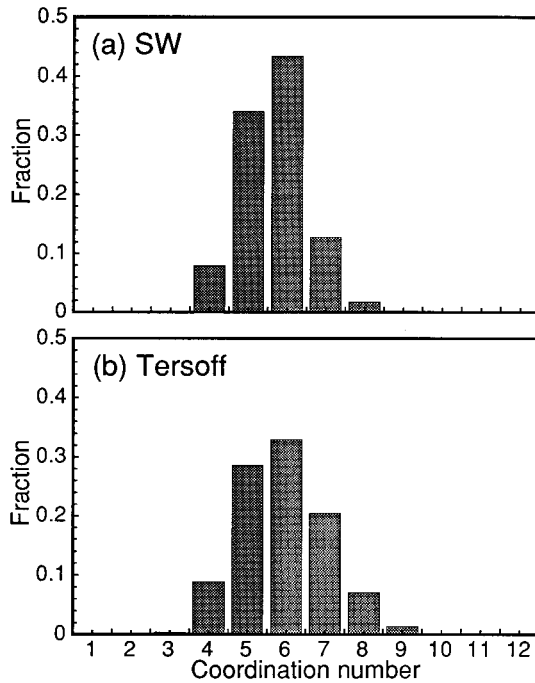


FIG. 3. Distribution of local coordination numbers in *l*-Si. (a) SW potential and (b) Tersoff potential. The coordination shells of (a) and (b) are defined by the first minimum of $g(r)$ and 3.1 Å, respectively.

of molten semiconductors.^{14,15,20,21} The shoulder appears in the large- k region of the main peak in (a), in accordance with the experiment.¹⁴ On the other hand, the shoulder appears in the small- k region in (b). This difference is due to the quantitative difference of $g(r)$ described in Fig. 1. It should be noted that the peak shape shown in Fig. 2(b) is similar to that of $S(k)$ for a supercooled liquid.¹⁵

The average coordination number, which is estimated by integrating $4\pi r^2 \rho_0 g(r)$ up to the first minimum in the $g(r)$, is 5.9 for the SW liquid and 5.2 for the Tersoff liquid. The former is close to the experimental value of 6.4,¹⁴ while the latter is appreciably small. The first minimum in $g(r)$ of the Tersoff liquid appears at 2.94 Å, which is shorter than that of *ab initio* MD simulation (3.1 Å).¹⁵ When the value 3.1 Å is applied, the coordination number of the Tersoff liquid becomes 6.0. Therefore, we use this cutoff distance for the following structural analyses of the Tersoff liquid, including the distribution of coordination numbers and bond-angle distribution function.

Figure 3 displays the distribution of coordination numbers in the *l*-Si. It can be seen that the coordination distributions are broad and centered around 6. The distribution is almost symmetric around the sixfold coordination in Fig. 3(b), while the fraction of the higher coordination numbers sharply decrease in Fig. 3(a). The coordination distribution of the Tersoff liquid resembles that reported by Štich, Car, and Parrinello.¹⁵

The bond-angle distribution functions $g(\theta)$ are shown in Fig. 4. The distribution is an average over 500 configurations during $500\Delta t$ (1 ps). A significant qualitative difference exists between (a) and (b). The SW liquid has a peak around 90°, while the Tersoff one has two peaks around 60° and 90°.

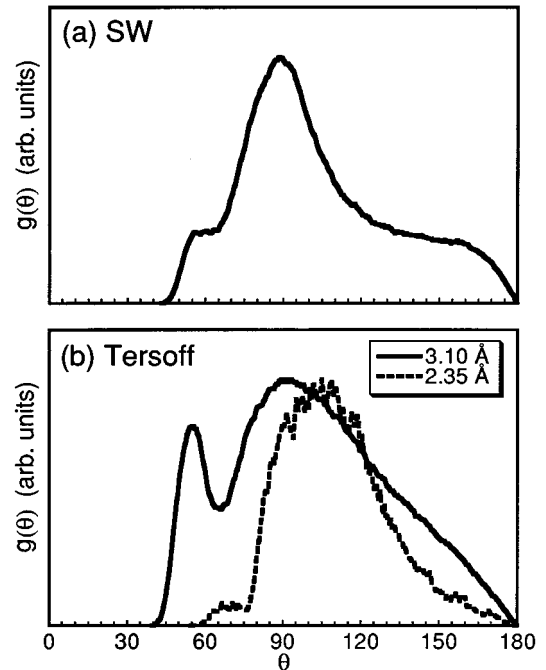


FIG. 4. Bond-angle distribution functions $g(\theta)$ in the atomic arrangements of (a) SW and (b) Tersoff liquid. In (b), solid and dashed lines are obtained by taking the bond lengths of 3.1 and 2.35 Å, respectively. It should be noted that the SW liquid has only one peak around 90°, while the Tersoff one has two peaks around 60° and 90°.

Although the Tersoff potential parameters do not fit to any liquid-phase data, the feature of $g(\theta)$ is in good agreement with that obtained by *ab initio* MD calculations.¹⁵ We must pay attention to the effects of simulation temperature on *l*-Si structure, because the Tersoff potential produces a melting point that is high by a factor of 2. However, even if the SW liquid is generated at 3000 K, the 60° peak does not appear (not shown). Therefore, it is concluded that the difference between Figs. 4(a) and 4(b) does not originate from the temperature. The discrepancy of the SW liquid can be attributed to the inadequacy of its three-body interaction term. When θ deviates from the ideal tetrahedral angle (109.47°), the three-body term, which is zero in the diamond structure, increases monotonically in the SW potential. Especially, the increase is remarkable at low θ . Thus, the distorted structure with low θ cannot exist stably in the SW liquid.

The dashed line in Fig. 4(b) indicates the $g(\theta)$ obtained by assuming the cutoff distance to be the bond length of crystalline Si. It is obvious that the bond angles associated with shorter bonds broadly distribute around the tetrahedral angle, while longer bonds form angle distributions around $\theta=60^\circ$ and 90° . The result is consistent with Štich's one corresponding to the bond length of 2.49 Å,¹⁵ indicating the validity of the Tersoff liquid. In the Tersoff potential, the bonding energy becomes weaker as the coordination number increases. Therefore, the bond angle around 60° can be considered to originate from the atoms with large coordination numbers.

Our simulated results obtained in this section support that the empirical interatomic potential established by Tersoff can qualitatively reproduce the static features of *l*-Si, though

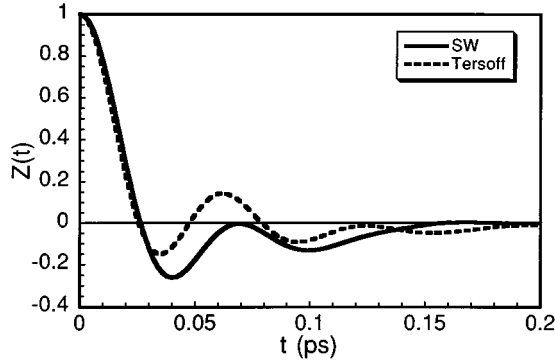


FIG. 5. Velocity autocorrelation functions $Z(t)$ for SW (solid line) and Tersoff liquids (broken line). For the SW liquid the $Z(t)$ becomes negative already at the first oscillation. On the other hand, it oscillates between positive and negative in the case of the Tersoff liquid.

there is a slight quantitative difference. The quantitative difference may be improved by modifying the cutoff distance of this potential.

B. Dynamical properties of liquid Si

Figure 5 displays the velocity autocorrelation functions defined by

$$Z(t) = \frac{\langle \mathbf{v}(t) \cdot \mathbf{v}(0) \rangle}{\langle \mathbf{v}(0) \cdot \mathbf{v}(0) \rangle}. \quad (2)$$

Here, $\mathbf{v}(t)$ is the velocity vector of a particle at time t . The average in Eq. (2) was taken over all particles and over different starting times along the equilibrium MD trajectories. $Z(t)$ becomes zero beyond 0.2 ps. An oscillation with a period of about 0.07 and 0.06 ps exists in the SW and Tersoff models, respectively, and the period is shorter than that of *ab initio* calculations (~ 0.1 ps).^{15,22} It should be noted that the $Z(t)$ of the solid line has a negative tail, but the first peak of the broken line becomes positive. For close-packed liquids such as Ar and Na, $Z(t)$ becomes negative already at the first oscillation.²³ The result of the Tersoff liquid is entirely different from the behavior of the simple liquids, but it is similar to $Z(t)$ of the *l*-Si generated by *ab initio* MD methods.^{15,22}

The Fourier transform of $Z(t)$ defines the power spectrum of the autocorrelation function,

$$Z(\omega) = \int_0^{\infty} Z(t) \cos(\omega t) dt. \quad (3)$$

Figure 6 shows $Z(\omega)$ corresponding to Fig. 5. According to the previous *ab initio* MD simulation,¹⁵ $Z(\omega)$ monotonically decreases with an increase of ω . However, two broad peaks appear in Fig. 6. The peaks in $Z(\omega)$ of the SW liquid correspond to the acoustic and optical vibrational modes of *c*-Si.¹⁵ On the other hand, $Z(\omega)$ of the Tersoff liquid possesses an intermediate nature between the *l*-Si generated by the SW potential and *ab initio* approach.

We have found that the Tersoff empirical potential yields the similar dynamical properties to those obtained by the

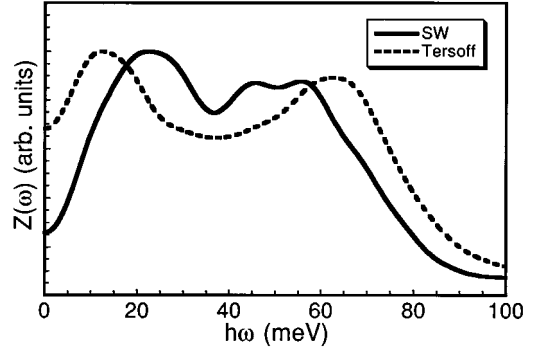


FIG. 6. Power spectra $Z(\omega)$ corresponding to Fig. 5. SW (solid line) and Tersoff liquids (broken line). The value of $Z(\omega)$ beyond $\omega = 100$ meV remains finite due to the short periodicity of $Z(t)$.

ab initio approaches, though some slight differences exist, e.g., the period of oscillation in $Z(t)$. This suggests that the interatomic forces obtained from this empirical potential are stronger than those of *ab initio* calculation.

IV. DISCUSSION

As mentioned in Sec. III A, a weak point of the Tersoff potential seems to be in its short-cutoff distance. We try to modify this potential through changing the cutoff distance. The parameters of the cutoff function were set to be $R = 3.0$ Å and $S = 3.3$ Å. [The original parameters are $R = 2.7$ Å and $S = 3.0$ Å (Ref. 16).] Unfortunately, the melting temperature in this case was 3500 K, which is higher than that of the original parameters (2750 K). Figure 7(a) shows $g(r)$ of atomic configurations obtained at 3700 K. As compared with Fig. 1(b), the first minimum of $g(r)$ in Fig. 7(a) is shallow, and its position appears at 3.12 Å. The average coordination number, as obtained by integrating $4\pi r^2 \rho_0 g(r)$ up to the first minimum, is 6.6. We can reproduce close value to the experiments¹⁴ without using the distance of the first minimum obtained by *ab initio* MD simulations.¹⁵ It should be noted that the value of the second peak maximum is almost 1 and it is smaller than that of the third peak maximum. This feature is in excellent agreement with the experimental data [Fig. 1(c)].

$S(k)$ corresponding to the $g(r)$ of Fig. 7(a) is given in Fig. 7(b). The first peak is asymmetric with a shoulder on the small- k region for the original parameters, as was shown in Fig. 2(b). However, such shoulder disappears in $S(k)$ of Fig. 7(b). This is considered to correspond to the intermediate state in which the shoulder moves from the small- k to large- k side of the main first peak. That is, $S(k)$ in Fig. 7(b) seems to be better than that obtained by the original cutoff distance. The distribution of coordination numbers and $g(\theta)$ obtained by new parameters are almost the same as Figs. 3(b) and 4(b), respectively (not shown). We could get better results for the static properties of *l*-Si through changing only the cutoff distance of the Tersoff potential.

Figure 8(a) demonstrates $Z(t)$ of *l*-Si generated by the modified Tersoff potential. For reference, $Z(t)$ of the original parameters is also indicated. Note that both simulated temperatures are the same (3700 K). An oscillation of a period

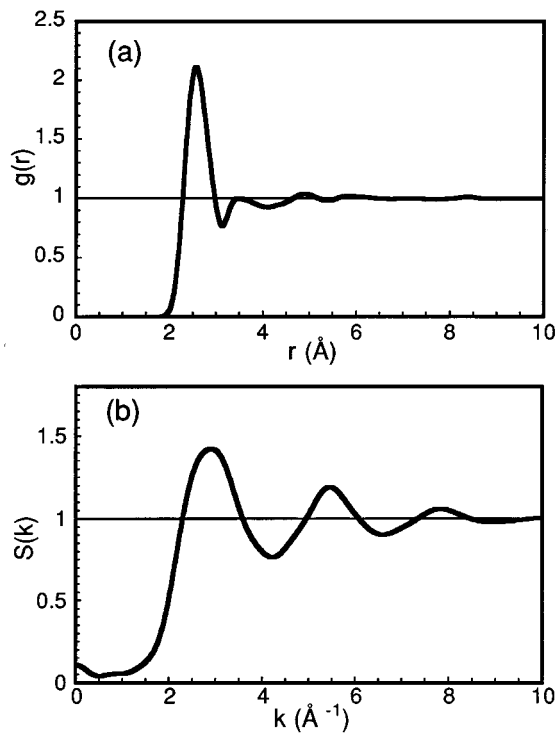


FIG. 7. (a) $g(r)$ and (b) $S(k)$ for l -Si resulting from the modified potential. Note that the second peak maximum in $g(r)$ is smaller than the third peak one.

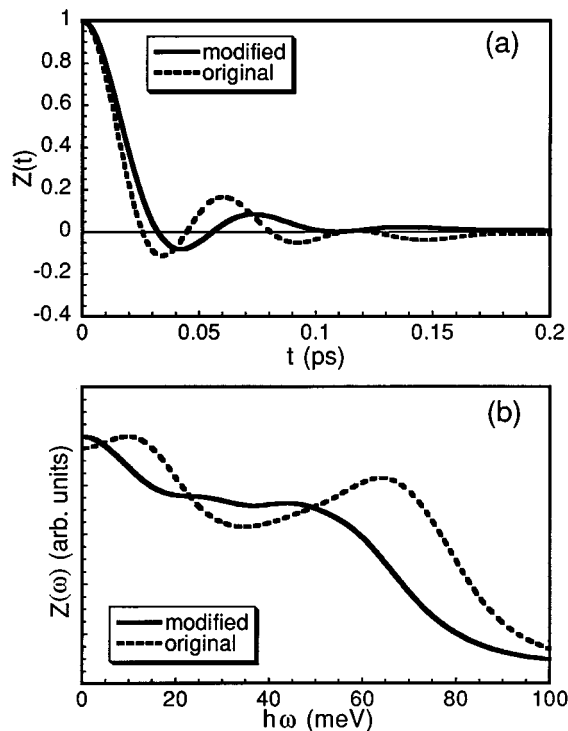


FIG. 8. (a) $Z(t)$ and (b) $Z(\omega)$ for l -Si generated by the original (broken line) and modified potential (solid line). The simulated temperature is 3700 K. In (a), it should be noted that the periodicity of the improved potential is longer than that of the original potential.

for the modified potential (solid line) is 0.075 ps. This value is larger than that for the original potential (broken line), but becomes close to the *ab initio* result.^{15,22} The result suggests that the longer cutoff distance weakens the forces acting on each particle in liquid. Corresponding $Z(\omega)$ is given in Fig. 8(b). The modified $Z(\omega)$ monotonically decreases with an increase in ω , and the humps appearing in the original $Z(\omega)$ disappear. Such a tendency in $Z(\omega)$ is in good agreement with that obtained by *ab initio* simulations.¹⁵ These results suggest that the change of cutoff distance is useful not only for the improvement of static properties, but also for a better description of the dynamic behavior.

Our improvement does not change the ground-state structure, and may not have bad effects on the elastic properties of c -Si which are determined by the curvature around the potential energy minimum. It should be necessary to find effective parameters to reduce the melting temperature in the Tersoff potential. The Tersoff potential has many adjustable parameters; thus we cannot say which parameter dominates the melting point at present. More extensive study is currently underway.

V. CONCLUSIONS

The empirical interatomic potentials constructed by SW and Tersoff were applied to the analyses of l -Si in order to examine the validity of both potentials. The findings of this investigation are as follows:

(1) The liquid obtained using the SW potential well reproduces the experimental $g(r)$ and $S(k)$. However, an important disagreement between the atomic arrangements resulting from the SW potential and the *ab initio* calculation method was found in the bond-angle distribution. The inadequate formula of the three-body interaction term gives rise to the discrepancy.

(2) Although the Tersoff potential does not fit any liquid-phase data, the qualitative features of static properties in the Tersoff liquid are in good agreement with those obtained by the experiments and *ab initio* MD simulations. Thus applications of this potential are promising for the analysis of l -Si.

(3) From the analyses of $Z(t)$ and $Z(\omega)$, it has been found that the SW empirical potential is not good enough for the description of l -Si. On the other hand, the $Z(t)$ and $Z(\omega)$ of the Tersoff liquid are similar to those of *ab initio* MD simulations, but some slight discrepancies exist.

(4) Our simulations suggested that successful results for the static structure and dynamical properties of l -Si are obtained through changing the cutoff distance of the Tersoff potential. More investigation must be carried out in order to reduce the melting temperature.

ACKNOWLEDGMENTS

We would like to thank T. Kumamoto for his help with the computer simulations. This work was partly supported by the New Energy and Industrial Technology Development Organization through the Japan Space Utilization Promotion Center.

- ¹H. Sasaki, E. Tokizaki, K. Terashima, and S. Kimura, *J. Cryst. Growth* **139**, 225 (1994).
- ²H. Sasaki, E. Tokizaki, K. Terashima, and S. Kimura, *Jpn. J. Appl. Phys.* **33**, 3803 (1994).
- ³R. Car and M. Parrinello, *Phys. Rev. Lett.* **55**, 2471 (1985); **60**, 204 (1988).
- ⁴F. H. Stillinger and T. A. Weber, *Phys. Rev. B* **31**, 5262 (1985).
- ⁵J. Tersoff, *Phys. Rev. B* **38**, 9902 (1988).
- ⁶R. Biswas and D. R. Hamann, *Phys. Rev. B* **36**, 6434 (1987).
- ⁷E. M. Peason, T. Takai, T. Holicioglu, and W. A. Tiller, *J. Cryst. Growth* **70**, 33 (1984).
- ⁸B. C. Bolding and H. C. Andersen, *Phys. Rev. B* **41**, 10 568 (1990).
- ⁹U. Landman, W. D. Luedtke, R. N. Barnett, C. L. Cleveland, and M. W. Ribarski, *Phys. Rev. Lett.* **56**, 155 (1986).
- ¹⁰Z. Q. Wang and D. Stroud, *J. Chem. Phys.* **94**, 3896 (1991).
- ¹¹S. J. Cook and P. Clancy, *Phys. Rev. B* **47**, 7686 (1993).
- ¹²K. Kakimoto, *J. Appl. Phys.* **77**, 4122 (1995).
- ¹³H. Ogawa and Y. Waseda, *Z. Naturforsch A* **49**, 987 (1994).
- ¹⁴Y. Waseda and K. Suzuki, *Z. Phys. B* **20**, 339 (1975).
- ¹⁵I. Štich, R. Car, and M. Parrinello, *Phys. Rev. B* **44**, 4262 (1991).
- ¹⁶J. Tersoff, *Phys. Rev. B* **39**, 5566 (1989).
- ¹⁷H. Balamane, T. Holicioglu, and W. A. Tiller, *Phys. Rev. B* **46**, 2250 (1992).
- ¹⁸K. Binder and D. W. Heerman, *Monte Carlo Simulation in Statistical Physics, An Introduction* (Springer, Berlin, 1988).
- ¹⁹J. Q. Broughton and X. P. Li, *Phys. Rev. B* **35**, 9120 (1987).
- ²⁰N. Takeuchi and I. L. Garzon, *Phys. Rev. B* **50**, 8342 (1994).
- ²¹G. Kresse and J. Hafner, *Phys. Rev. B* **49**, 14 251 (1994).
- ²²J. R. Chelikowsky, N. Troullier, and N. Binggeli, *Phys. Rev. B* **49**, 114 (1994).
- ²³J. P. Hansen and I. R. McDonald, *Theory of Simple Liquids* (Academic, London, 1976).